

Global experimental response of a three-story, full-scale precast concrete shear wall structure with reinforcing bars spliced by grouted couplers

Wenlong Han, Zuozhou Zhao, and Jiaru Qian

- This paper presents an experimental study of a three-story, full-scale precast concrete shear wall structure that was subjected to a series of pseudodynamic and quasi-static tests.
- Critical connections, such as horizontal and vertical wall-to-wall joints, window belly wall connections, slab-to-wall joints, slab-to-slab joints, and precast concrete sandwich panel connections, were designed and verified.
- Test results verified that the connections were strong enough to ensure that the test model behaved as if it were monolithic, and the global performance of the test model was comparable to that of cast-in-place concrete structures.

Compared with cast-in-place concrete construction, precast concrete construction contributes to better site control, accelerated construction, reduced on-site labor, and improved durability. This has resulted in an increased use of precast concrete structures in many seismic areas, especially in China during the past decade. However, precast concrete residential buildings in China are mostly designed as precast concrete shear wall structures rather than precast concrete frames, which, although commonplace in the West and Japan, has encountered great resistance in China.

Precast concrete wall systems can be classified as either jointed or equivalent monolithic systems. Jointed systems are designed with dry or ductile connections, such as bolted or welded steel plate connections,¹⁻³ energy dissipation devices,⁴ and prestressed rocking connections,⁵ so that damage occurs in the connections rather than in precast concrete members. With equivalent monolithic systems, dedicated reinforcing bar splices—such as grouted couplers,⁶ grouted corrugated pipe connections,⁷ pressed couplers,⁸ or bolted connections⁹—are used to achieve continuity between vertical reinforcing bars of adjacent upper and lower precast concrete walls. The grouted coupler transfers tensile and compressive forces through the deformed ribs of spliced reinforcement into the high-strength grout and then to the steel sleeve. Nowadays, embedment lengths of reinforcement have been shortened to six to eight times the spliced reinforcing bar diameter d in grouted couplers. This is because the grouted couplers have been optimized by bolts,¹⁰

PCI Journal (ISSN 0887-9672) V. 64, No. 1, January–February 2019.

PCI Journal is published bimonthly by the Precast/Prestressed Concrete Institute, 200 W. Adams St., Suite 2100, Chicago, IL 60606.

Copyright © 2019, Precast/Prestressed Concrete Institute. The Precast/Prestressed Concrete Institute is not responsible for statements made by authors of papers in *PCI Journal*. Original manuscripts and discussion on published papers are accepted on review in accordance with the Precast/Prestressed Concrete Institute's peer-review process. No payment is offered.

welded reinforcing bars,¹¹ tapered shapes,¹² or shear keys¹³ to enhance the bond strength and achieve more efficient connections. Note that the grouted coupler balances construction efficiency and mechanical performance, and it has become the most popular coupler used in precast concrete structures in China.

Vertical cast-in-place concrete segments¹⁴ are typically used to connect adjacent precast concrete walls in equivalent monolithic systems, and these segments are made overly strong to transmit interface forces. Considering that most residential buildings in China's major cities are 10- to 30-story high-rise buildings, Chinese precast concrete code¹⁵ recommends equivalent monolithic systems to achieve a large lateral stiffness and good integrity. An emulative precast concrete shear wall system with grouted couplers (**Fig. 1**) consists of the following:

- Wall vertical reinforcing bars are spliced by grouted couplers.
- Adjacent precast concrete panels are connected by vertical segments.
- Precast concrete slabs with cast-in-place concrete toppings are used as diaphragms tying vertical members together.

This system has attracted many scholars' and engineers' attention in China. The performance of precast concrete walls, coupling beams, and coupled walls in precast concrete shear wall system with grouted couplers have been thoroughly discussed in recent years.

Previous research indicated that precast concrete walls with single-layer reinforcement mesh and single-row spliced vertical reinforcing bars exhibited significant rocking under lateral loads—that is, damage concentrated on horizontal joints, characterized by visible shear slip, gap opening, and concrete crushing rather than well-distributed plastic hinges.^{1,16} Meanwhile, these precast concrete walls performed poorly under out-of-plane loads.¹⁷ Note that these precast concrete walls with poor strength, stiffness, and energy dissipation capacity are not suitable for high-rise buildings.

Precast concrete walls with a double-layer of mesh reinforcement and boundary elements are recommended in China, resulting in stronger reinforcement connections between the upper and lower floors. Test results showed that precast concrete walls with Chinese reinforcement details and reinforcing bars spliced by grouted couplers exhibited overall behavior, strength, energy dissipation, and deformation capacity that were comparable to cast-in-place concrete walls.^{18–21} In addition, the details—with boundary element reinforcing bars were each spliced by grouted couplers and the vertical, distributed reinforcing bars indirectly lapped by single-row additional reinforcing bars—were proposed to lower the cost of reinforcing bar splices.^{20–22} Tests on vertical wall-to-wall joints demonstrated that cast-in-place segments could satisfactorily connect the precast concrete panels failing in flexural

modes and that the rough surface was more suitable than the shear key due to better cracking resistance.¹⁸

Coupling beams show an important role in energy dissipation of shear wall structures. In a precast concrete shear wall system with grouted couplers, coupling beams are designed as superimposed members for precast concrete construction, which consist of precast concrete beams and cast-in-place concrete toppings that simultaneously serve as slab-to-wall joints. Tests on superimposed coupling beams²³ and coupled walls^{22,24} indicated that connections between the precast concrete beams and cast-in-place concrete toppings were strong enough to emulate coupling beams. Compared with coupling beams precast individually from wall piers, coupling beams precast with wall piers as a whole exhibited better joint performance.

As described, seismic performance of single elements in the precast concrete shear wall system with grouted couplers—such as precast concrete walls, coupling beams, and coupled walls—has been thoroughly determined experimentally.^{18–24} However, for an overall structure of this kind, its performance and, in particular, its response to seismic excitation has not been thoroughly investigated at present. In this study, a 16-story prototype structure using precast concrete shear wall system with grouted couplers was designed in accordance with Chinese codes. Then, a three-story, full-scale substructure of the prototype was constructed and subjected to a series of pseudo-dynamic and quasi-static tests. This paper investigates the response and damage states of the structure under earthquakes of different intensities, as well as several areas of concern in the design and construction of precast concrete shear wall systems with grouted couplers, including the following:

- performance of joints connecting precast concrete members
- influence of window belly walls that were precast together with wall piers
- performance of precast concrete sandwich walls
- performance of superimposed concrete slabs with different slab-to-wall joints

Test model and parameters

Considering the loading capacity of actuators and spatial limitations of the test site, a three-story substructure of a 16-story prototype structure was chosen as the test model to investigate the seismic performance of precast concrete shear wall systems with grouted couplers. The prototype was designed following current Chinese code GB 50011-2010²⁵ for seismic design of buildings and code GB 50010-2010,²⁶ for the design of concrete buildings and located on a site with seismic design intensity 8 (the maximum spectral acceleration was 0.20g for 10% probability of exceedance in 50 years, where g is the acceleration due to gravity). The prototype had a total height of 48 m (157.5 ft) with a floor-to-floor height

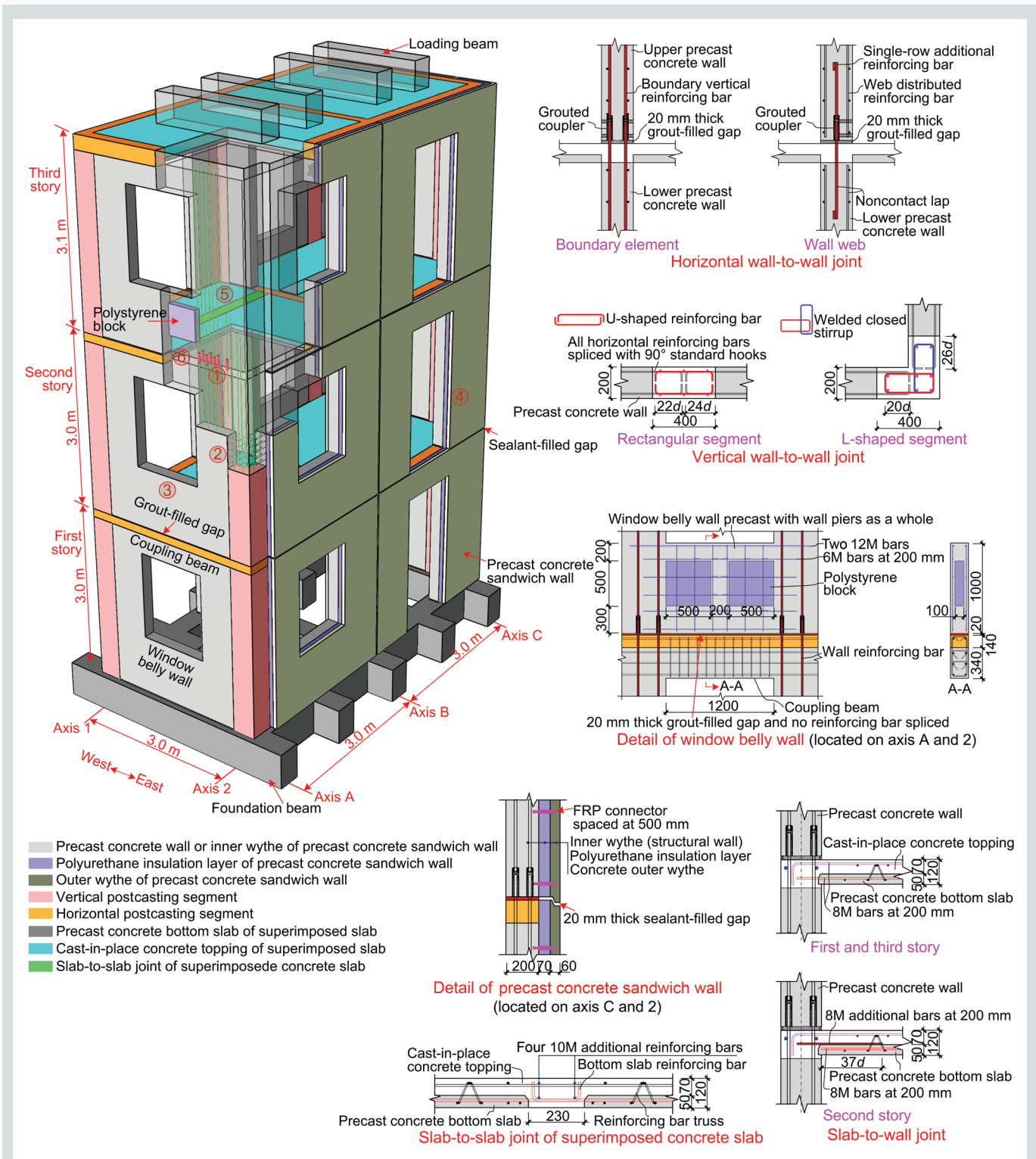


Figure 1. Test model. Note: units in are in millimeters unless indicated otherwise. d = reinforcing bar diameter; FRP = fiber-reinforced polymer. 6M = no. 2; 8M = no. 3; 10M = no. 4; 12M = no. 5; 20M = no. 6; 1 mm = 0.0394 in.; 1 m = 3.2808 ft.

equal to 3 m (9.8 ft). The test model (Fig. 1) was 3 × 6 m (9.8 × 19.7 ft) in plan, with story heights, wall thicknesses, coupling beam heights, coupling beam spans, slab thicknesses, material strength, and reinforcement arrangement identical to the prototype. A detailed description of the geometry and reinforcement details of the test model and the prototype is given in a companion research report.²⁷

Horizontal wall-to-wall joint

In actual projects, walls in a precast concrete shear wall systems with grouted couplers are divided and precast by story with consideration of the transport and erection methods. In precast concrete walls, boundary-element longitudinal rein-

forcing bars were each spliced by threaded grouted couplers while web vertical distributed reinforcing bars were indirectly lapped by single-row additional reinforcing bars that were spliced by threaded grouted couplers. The diameter of the additional reinforcing bar was determined by the principle that the additional reinforcing bar area should not be less than the vertical distributed reinforcement area. Longitudinal reinforcing bars of the lower-story precast concrete wall protruded into the corresponding grouted sleeves of the upper-story precast concrete wall. After erecting the upper precast concrete wall, threaded couplers were grouted with high-strength grout, forming a 20 mm (0.8 in.) high grout-filled construction gap below the precast concrete wall (Fig. 1). The measured compressive strength of grout for the first, second, and third story was 112.9, 101.1, and 90.5 MPa (16.4, 14.7, and 13.1 ksi), respectively, higher than the design required value of 80 MPa (11.6 ksi).

Vertical wall-to-wall joint

Walls of each story were divided into seven precast concrete panels in accordance with actual projects. Vertical cast-in-place segments with rectangular, L-shaped, or T-shaped cross sections were used to connect precast concrete panels vertically. Rectangular vertical joints were located at wall web zones, while L-shaped or T-shaped vertical joints were located at boundary element zones.

As illustrated in Fig. 1, horizontal reinforcing bars protruding from adjacent precast concrete panels and with 90-degree standard hooks were lapped by additional U-shaped reinforcing bars or welded closed stirrups. These vertical joint details are convenient to construct because the reinforcing bars do not overlap and there is greater ease lowering the precast concrete panels over starter reinforcing bars. The specification and spacing of protruding horizontal reinforcing bars and additional reinforcement were the same as precast concrete wall horizontally distributed reinforcing bars. In addition, vertical reinforcing bars in cast-in-place segments enhance the connection strength. The sides of the precast concrete walls were rough surfaces on which concrete aggregate was exposed by water jetting to postpone cracking of the interface between vertical cast-in-place segments and precast concrete walls.¹⁸ The performance of vertical cast-in-place segments was specially identified in this study.

Detail of window belly wall

In Chinese cast-in-place concrete structures, window belly walls are usually designed as nonstructural components and constructed by bricks or aerated concrete blocks after the main structure is completed. The contribution of window belly walls is neglected in the design of this kind of structure. For precast concrete shear wall with systems grouted couplers, window belly walls are generally precast with wall piers as a whole to achieve an integrated architectural facade and higher construction quality. This study proposed novel construction details to weaken the window belly wall influence. As shown

in Fig. 1, for window belly walls located on axes A and 2 (1000 mm [39.4 in.] high), polystyrene blocks were introduced to decrease the stiffness of window belly walls. The height of window belly walls located on axes C and 1 was too small (400 mm [15.7 in.] high) to place polystyrene blocks, so these window belly walls were solid concrete walls reinforced with constructional reinforcement.

All window belly walls and the lower horizontal cast-in-place segments were connected by 20 mm (0.8 in.) thick, high-strength-grout-filled construction gaps with no spliced reinforcement. Note that the connections between the window belly wall and the shear wall or the lower coupling beam in precast concrete shear wall systems with grouted couplers are stronger than those in cast-in-place concrete systems, so the influence of window belly walls on the seismic behavior of precast concrete shear wall systems with grouted couplers was investigated in this study.

Precast concrete sandwich wall connections

Precast concrete sandwich walls with a 60 mm (2.4 in.) thick concrete outer wythe, 70 mm (2.8 in.) thick polyurethane insulation layer, and 200 mm (7.9 in.) thick concrete inner wythe, were adopted as exterior walls of axes C and 2. The outer and inner wythes were fastened to each other by fiber-reinforced polymer (FRP) connectors spaced at 500 mm (19.7 in.). Inner wythes (structural walls) of adjacent precast concrete sandwich walls were connected to each other by horizontal or vertical wall-to-wall joints, while adjacent outer wythes were not connected and were separated by 20 mm (0.8 in.) wide sealant-filled gaps. The performance of precast concrete sandwich walls, especially the outer wythe influence, was investigated in this study.

Slab-to-wall and slab-to-slab joints

Two-way superimposed concrete slabs with 50 mm (2.0 in.) thick precast concrete bottom slabs and 70 mm (2.8 in.) thick cast-in-place concrete toppings were used as the first- and second-story floors of the test model, while two-way superimposed concrete slabs with 50 mm (2.0 in.) thick precast concrete bottom slabs and 150 mm (5.9 in.) thick cast-in-place concrete toppings were used as the third-story floor to enhance the loading setup, which was mounted on top of the test model.

Different slab-to-wall joints (that is, floor connections)—namely, connections with protruding reinforcing bars and connections without protruding reinforcing bars—were designed and verified in the test model (Fig. 1). For connections with protruding reinforcing bars (used in the first and third floors), longitudinal reinforcing bars in the precast concrete bottom slab protruded from the slab sides and were embedded in horizontal cast-in-place segments above walls, resembling reinforcement details of slab-to-wall joints in cast-in-place concrete structures. In actual projects, connections with

protruding reinforcing bars may lead to inefficient erection and poor quality due to these protruding reinforcing bars. To overcome this problem, the second floor was equipped with a connection without protruding reinforcing bars, in which no reinforcing bar protruded from the sides of the precast concrete bottom slab, and additional reinforcing bars with diameter and spacing identical to precast concrete slab longitudinal reinforcing bars were placed at the top of the precast concrete bottom slabs. The continuity of bottom longitudinal reinforcement of slabs, which is achieved in conventional cast-in-place concrete slabs and superimposed slabs with protruding reinforcing bars, provides diaphragms with a high degree of integrity. However, considering the discontinuity of precast concrete slab longitudinal reinforcement, it is unclear whether floors that are connected without protruding reinforcing bars can behave as a diaphragm in emulated floors that are connected with protruding reinforcing bars resisting gravity loads, as well as tying the lateral-force-resisting members together and distributing lateral forces arising from wind and seismic actions.

Considering cracking control and transport, it is impractical to prefabricate oversized bottom slabs (50 to 70 mm [2.0 to 2.8 in.] thick) for large rooms. Thus, precast concrete bottom slabs of large rooms must inevitably be divided into small slabs. To simulate the split condition of large floors in actual projects, precast concrete bottom slabs of the first and second story between axes A and B were divided into two parts, which were connected by a 230 mm (9.1 in.) wide cast-in-place concrete monolithic segment (Fig. 1). The segment was located at $\frac{1}{3}$ span of the floor, and reinforcing bars protruding from the sides of precast concrete slabs were anchored into the segment.

Experimental program

Figure A1 shows the test setup, where the foundation beam of the test model was securely clamped to the reaction floor (for appendix figures, go to <https://www.pci.org/2019Jan-Appx>). The axial load, with a total value of 14,890 kN (3347 kip) and a design axial force ratio of 0.40, was applied to wall piers by prestressing tendons. Slabs of the first and second stories were stacked with iron blocks weighing 2.0 kN/m² (0.3 psi) to simulate gravity loads on floors. Cyclic lateral loads were applied in the east-west direction by four actuators, which were horizontally mounted to the loading beams at the model top. The push eastward was defined as the positive load and the pull westward as the negative load.

All of the tests consisted of pseudodynamic and quasi-static tests. The substructure pseudodynamic method developed at the structure laboratory of Tsinghua University in Beijing, China, was used for the pseudodynamic tests.²⁸ As depicted in **Fig. A2**, the upper 13 stories of the 16-story prototype, implemented as the simulated substructure, were simplified to a five-degree-of-freedom mass-spring system and simulated on the computer; meanwhile, the bottom three stories, designated as the experimental substructure, were simplified to a one-degree of freedom system and subjected to physical testing in the laboratory. During the pseudodynamic tests, the

displacements were calculated from the simplified model. Those displacements were scaled using a similarity relation and applied to the test model to obtain the lateral forces in the top of the test model. The lateral forces in the test model were then scaled, again using a similarity relation, and applied to the simplified model. This process was repeated to get each loading step.

The first 25 seconds of the Taft 1952 east-west (EW) earthquake record, with a peak ground acceleration (PGA) of 175.9 cm/sec² (5.8 ft/sec²), was used as the input motion in a series of pseudodynamic tests in which the seismic intensity gradually increased. The accelerogram was scaled to the chosen PGA:

- 0.035g for frequent earthquakes (63.5% probability of exceedance in 50 years) of seismic fortification intensity 7
- 0.07g for frequent earthquakes of seismic fortification intensity 8
- 0.20g for precautionary earthquakes (10% probability of exceedance in 50 years) of seismic fortification intensity 8
- 0.40g for rare earthquakes (2% to 3% probability of exceedance in 50 years, that is, maximum considered earthquake) of seismic fortification intensity 8
- 0.62g for rare earthquakes of seismic fortification intensity 9²⁵

To approach the ultimate capacity of the test model, a final quasi-static test was conducted after the pseudodynamic tests, controlling the top drift ratio θ of the model. The loading protocol for the pseudodynamic and quasi-static tests is depicted in **Fig. A3**.

Validation of test method

Influence of prestressing force

As described, the large axial load N was applied by 28 groups of prestressing tendons, which might influence the test model stiffness and then affect the response under excitation, especially in pseudodynamic tests. The fundamental frequency of the test model was measured by the hammering method before and after tensioning. The results parallel and perpendicular to the earthquake input direction were 9.62 and 12.45 Hz before tensioning, respectively, while the corresponding values were 9.81 and 12.60 Hz after tensioning, which were less than a 2% increase. It can be concluded that tensioning prestressing tendons had little effect on the initial lateral stiffness of the test model.

The prestressing tendons, with anchoring ends fixed on the foundation beam and tensioning ends fixed on the third-story slab, would be tilted under lateral loads. A horizontal compo-

net F_H , which was opposite the lateral force F_A applied by actuators, would then be produced by tension forces of inclined prestressing tendons. Meanwhile, the length of prestressing tendons changed with the top lateral displacement of the test model resulting in a change of the prestressing force. The increment of the prestressing force ΔN was monitored by load cells during testing. F_H can be calculated by the relationship shown in **Fig. A4** and written as the following:

$$F_H = (N + \Delta N) \times \sin[\arctan(u/L_0)]$$

where

L_0 = initial length of prestressing tendons

u = lateral displacement of the third-story slab

Figure A4 shows the relationship between the maximum lateral force $F_{A,max}$ applied by actuators and the corresponding F_H during testing. The prestress had little effect on the lateral force in pseudodynamic tests, with relative force δ less than 5%, revealing that it was reasonable to neglect the influence of F_H when considering the returning force obtained from the experimental substructure to the simplified model for dynamic calculation. Relative force δ increased with the top displacement increasing, with a value larger than 15% at $1/50$ drift. Hence, F_H should be considered in the calculation of the base shear force F_{EK} .

Response in pseudodynamic tests

Inevitable gaps and elastic deformation of connectors for actuators may affect the loading accuracy in pseudodynamic tests, especially for test models with large stiffness, as in this paper. In addition, cumulative loading errors may result in a rather different response of the test model. To accurately evaluate the seismic performance of the test model, the actual outer displacement Δ of the loading beams was used as the displacement feedback for input to the pseudodynamic tests.

The lateral displacement Δ was measured by two high-precision displacement transducers (DTs) mounted at the loading beams. **Figure 2** plots the displacement responses in the 0.07g and 0.62g pseudodynamic tests, where “desired displacement” denotes the target applied displacement of the loading beams, “DT displacement” is the actual outer displacement Δ measured by the outer DTs, “actuator displacement” denotes the displacement measured by the internal DT of the actuator, and “slippage” is the slippage of the foundation beam. Figure 2 shows that DT displacement almost coincided with desired displacement, while a significant difference existed in actuator displacement. This indicates that the gaps and elastic deformation of connectors for actuators, which were included in actuator displacement, were fairly large. If actuator displacement were used as the displacement feedback in pseudodynamic tests, the actual displacement of the test model (DT displacement) would be different from the desired displacement, resulting in a garbled seismic response. Considering that the slippage of

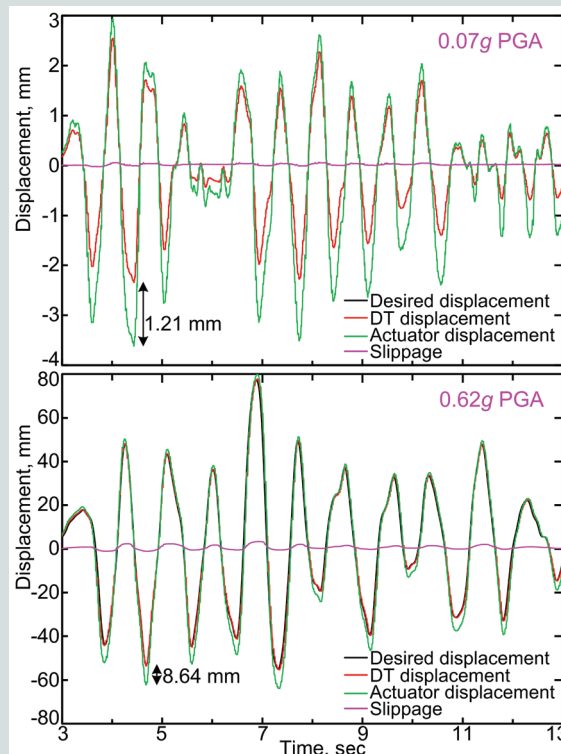


Figure 2. Displacement time-history curves in pseudodynamic tests. Note: DT = displacement transducer; g = acceleration due to gravity; PGA = peak ground acceleration. 1 mm = 0.0394 in.

the foundation beam was rather small compared with lateral displacement at loading beams Δ in pseudodynamic tests (**Fig. 2**), pseudodynamic tests controlled by DT displacement could accurately emulate the seismic response of the test model, which is discussed in the next section of this paper.

Test results and discussion

Test observation

Failure mode of test model After the first cycle of $1/50$ drift, the quasi-static test was terminated for safety reasons. As shown in **Fig. A5**, cracks and damage in the test model concentrated on the coupling beams and window belly walls in the east-west direction, characterized by severe cracking and concrete spalling, while cracks of wall piers distributed at a height of 0 to 2.0 m (0 to 6.6 ft) from the foundation with a maximum width of 2 mm (0.08 in.) and no crack was observed at the wall piers of the second and third stories. The test model exhibited the desired “strong wall pier and weak coupling beam” failure mode.

Performance of wall-to-wall joints At $1/120$ drift (the elastoplastic interstory drift limit for shear wall structures stipulated in Chinese codes) of the quasi-static test, a 2.5 mm (0.10 in.) wide opening formed at the grout-filled foundation-to-wall construction gap, while the maximum crack width of walls was 1.0 mm (0.04 in.). After $1/120$ drift, more cracks devel-

oped at wall piers and previous cracks widened. The inelastic deformation of precast concrete walls was dominated by the well-distributed cracks in the wall bottom (Fig. A5) rather than the horizontal foundation-to-wall joint opening. Visible gap opening and shear slip at horizontal joints, which were observed in tests of other types of precast concrete shear walls,^{1,16} did not occur during the test. **Figure 3** shows the strains of the boundary element longitudinal reinforcing bar (each spliced by threaded grouted coupler) and the web vertically distributed reinforcing bar (indirectly lapped by a single-row of additional reinforcing bar) during the test, where the strain gauges were mounted above the sleeves. Strains of reinforcing bars spliced by threaded grouted couplers increased with the lateral load increasing and no abrupt strain decrease was observed, indicating that the threaded grouted coupler could transfer the force of the spliced reinforcing bars effectively.

Figure A6 shows the cracks and damages around vertical wall-to-wall joints. Cracks in the precast concrete walls could continuously develop into the vertical cast-in-place segments, and no damage occurred at the interface between the cast-in-place segment and precast concrete wall, indicating that vertical joints connecting adjacent precast concrete walls were strong enough to ensure the behavior of walls as if monolithic. The previously mentioned observations validated the reliability of the proposed horizontal and vertical wall-to-wall joints.

Influence of window belly walls After the 0.40g pseudo-dynamic test, all coupling beams were dominated by flexural cracks, while shear cracks developed at the window belly walls located on axes A and C at the second and third stories (**Fig. 4**). Two long vertical cracks formed around the polystyrene filling blocks in window belly walls on axis A. As the top lateral displacement increased, shear cracks on window belly walls developed rapidly. After the quasi-static test, the window belly walls on axes A and C failed in shear mode, characterized by visible inclined cracks and spalling of cover concrete. Influenced by the upper window belly walls, coupling beams located on axes A and C at the first and second stories, with aspect ratios of 2.5, were mainly dominated by shear-inclined cracks. Continuous diagonal cracks ran through the upper window belly walls and lower coupling beams while coupling beams sank and window belly walls sagged under the inclined compression, indicating that the upper window belly walls and lower coupling beams worked together to resist shear and moment under large drift (**Fig. 4**).

Conversely, coupling beams located on axes A and C at the third story, with aspect ratios of 2.1 and no upper window belly wall, failed in flexural mode, characterized by concentrated plastic hinges at both ends and slight shear cracks (**Fig. 4**). The crack pattern difference between coupling beams with or without window belly walls indicated that the upper window belly walls significantly influenced the crack distribution of coupling beams and a composite effect existed in the lower coupling beam and upper window belly wall, though weak construction details, such as infilling polystyrene blocks in window belly walls or no spliced reinforcement between

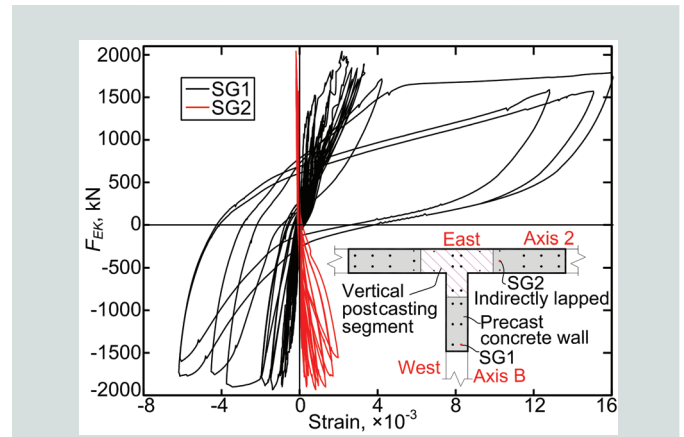


Figure 3. Vertical reinforcing bar strain response versus base shear. Note: F_{EK} = base shear force. 1 kN = 0.225 kip.

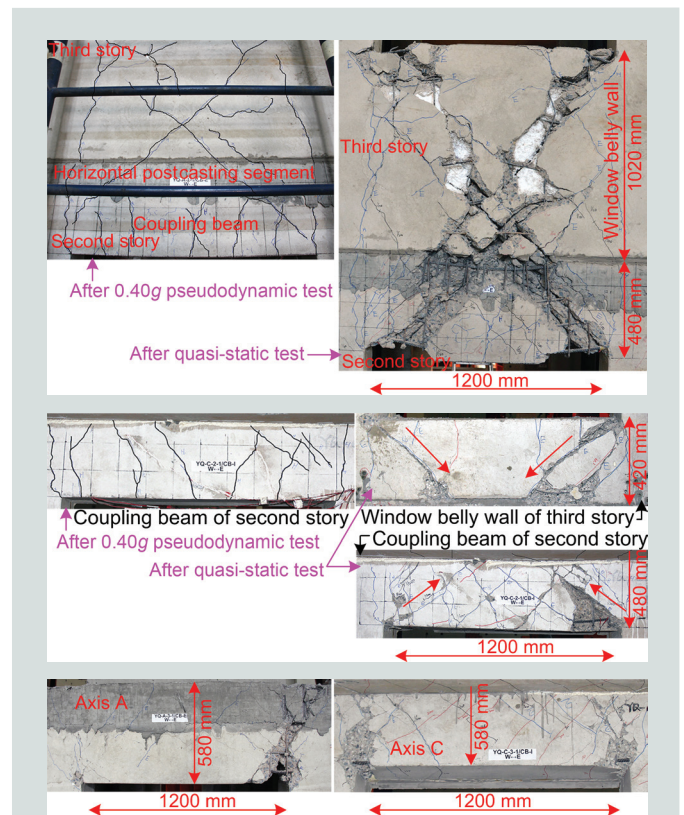


Figure 4. Failure modes of coupling beams and window belly walls. Note: g = acceleration due to gravity. 1 mm = 0.0394 in.

coupling beams and window belly walls, were evident. In addition, no damage occurred at the connections between the window belly wall and adjacent precast concrete wall piers. Additional studies might be necessary to identify the influence of the window belly wall on the stiffness and failure mode of the structure, which should be carefully considered in structure design. Considering that it may be difficult to balance the architectural and structural requirements, designing the window belly wall as an upper coupling beam to form double coupling beams²⁹ in precast concrete shear wall systems with grouted couplers may be a feasible alternative.

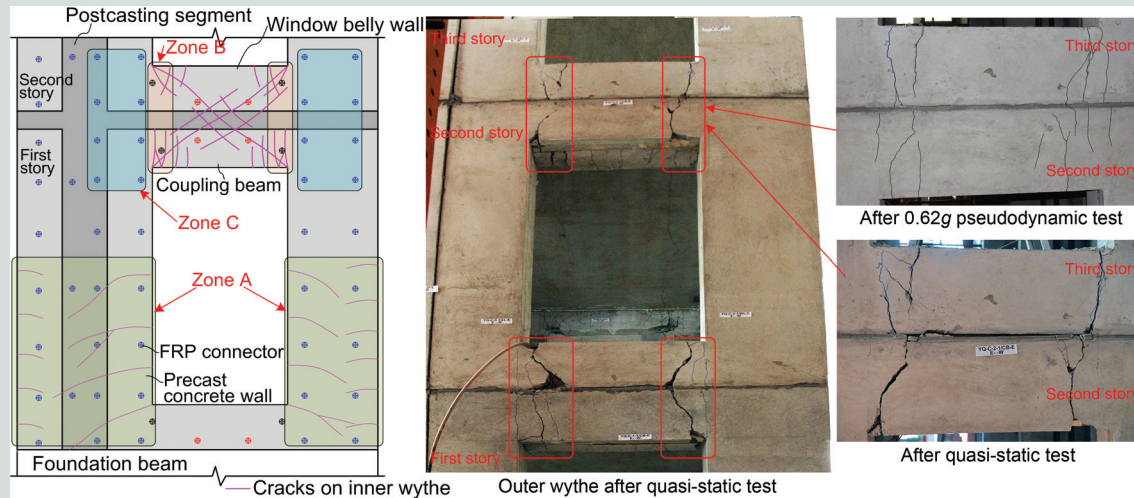


Figure 5. Failure mode of the outer wythe of precast concrete shear walls on axis C. Note: FRP = fiber-reinforced polymer; g = acceleration due to gravity.

Performance of precast concrete sandwich walls Damage to the outer wythes of the precast concrete sandwich walls on axis C concentrated in zones corresponding to coupling beams and window belly walls. Damage was characterized by visible vertical cracks concentrating at both ends (Fig. 5), while several hairline cracks formed at zones corresponding to wall piers at the first story. The crack distribution and pattern of the outer wythe were distinctly different from those of the inner wythe (Fig. A5 and 4), revealing that the stress states of the outer and inner wythes were not identical, which can be explained by Fig. 5. The outer and inner wythes were fastened to each other by FRP connectors, which were not rigidly connected and could dissipate a certain deformation of the inner wythe instead of transmitting it directly to the outer wythe. The wall piers of the inner wythe at the first story suffered slight well-distributed cracking (plastic deformation), which could be dissipated by the deformation of FRP connectors; hence no visible crack formed at corresponding zones of the outer wythe (zone A in Fig. 5).

As mentioned, damage to the test model concentrated on coupling beams and window belly walls, which underwent large plastic deformation. In addition, the material contribution due to residual tensile reinforcing bar strains and shear dilatancy of concrete and the “geometrical contribution” due to the section rotation resulted in the axial length of the coupling beams elongating during cyclic loading, which is well known as beam elongation.³⁰ Previous studies showed that this elongation could reach 2% to 5% of the beam depth at each plastic hinge.³¹ FRP connectors in these zones could not completely dissipate these large plastic deformations due to the constraint of FRP connectors in zone C; therefore, visible vertical cracks were concentrated in zone B of the outer wythe (Fig. 5). A low degree of in-plane composite action between the outer and inner wythes was achieved by using FRP connectors, especially under small deformation, indicating that the influence of the outer wythe can be neglected in structure design. Note that vertical cracks in the outer wythe run through the whole

section depth, leading the outer wythes between beam ends to act independently, requiring that reinforcing bars running through the vertical cracks and FRP connectors between these cracks (the red dots in Fig. 5) should be well designed and detailed to prevent falling of the independent part of the outer wythe under large drift. After the tests and removal of the outer wythe, no damage was observed on the FRP connectors, validating the reliability of the connection details adopted in the precast concrete sandwich walls.

Performance of superimposed slabs The strains in the slab negative reinforcement (SNR) of the cast-in-place concrete topping along slab-to-wall joints were measured during the testing. According to the internal force distribution under vertical and lateral loads, the tension strains of the slab bottom longitudinal reinforcing bars were comparable to or less than those of the SNR. Under the serviceability limit state (that is, the axial load on walls and gravity load on floors were applied), 0.07g PGA, and 0.20g PGA, the maximum tension strains in the SNR were 79, 88, and 179 $\mu\epsilon$, respectively, which were less than concrete cracking strain (twice the peak strain of concrete under uniform tension³²), indicating that there was no significant difference between the performance of connections with protruding reinforcing bars and connections without protruding reinforcing bars under these loading states.

The maximum tension strain in the SNR increased significantly under 0.42g and 0.62g PGA, with values of 1783 and 2993 $\mu\epsilon$, respectively, and SNR yielded by tension under 0.62g PGA. After the quasi-static test, no visible cracking or slippage was observed around the connections with protruding reinforcing bars or the connections without protruding reinforcing bars (Fig. 6). Meanwhile, the two measured lateral displacements on axes A and C at the same story were approximately identical, showing that the test model moved as a stiff body and torsion in the floor plane could be negligible. A superimposed slab without protruding reinforcing bars can work as a diaphragm emulated to slab with protruding reinforcing

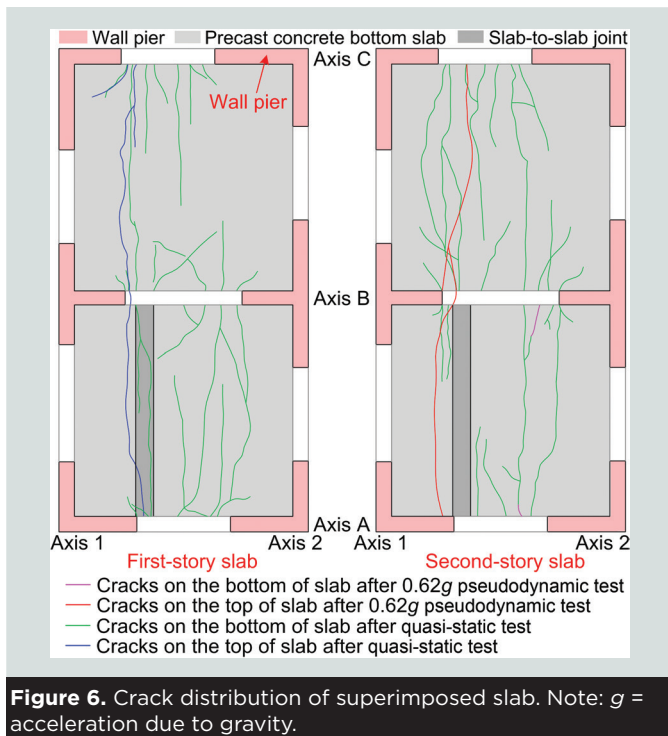


Figure 6. Crack distribution of superimposed slab. Note: g = acceleration due to gravity.

bars, resisting gravity loads as well as tying lateral-force-resisting members together and distributing lateral forces.

As shown in Fig. 6, a set of cracks perpendicular to lateral loads formed at the tops and bottoms of slabs and distributed along coupling beams. In particular, some of these cracks ran through the two bays in the north-south direction. Three factors contributed to the slab cracking:

- The slab worked as the flange of the coupling beam to resist moments.
- The coupling beam sank due to the inclined compression.
- The coupling beam elongated under cyclic loading.

These three factors were limited within the coupling beam span due to the constraint effect from adjacent long and large-stiffness wall piers, which significantly decreased plastic tension deformation around slab-to-wall joints. Therefore, extensive cracking along beams³³ and unseating failure of

slabs³⁴ in precast concrete frames, which result in the loss of gravity support and diaphragm action of the floor, did not occur in this study. The constraint effect from wall piers made important contributions to ensuring the gravity support and diaphragm action of superimposed slab without protruding reinforcing bars. Therefore, wall piers should be designed with enough lateral stiffness to enhance the constraint effect in superimposed slabs without protruding reinforcing bars.

Force-displacement response

Figure A7 plots hysteresis curves or skeleton curves of the test model under different load conditions, where F_{EK} denotes the base shear force and the prestress influence was removed. Under 0.035g and 0.07g PGA, F_{EK} was linearly related to u , indicating that the test model suffered limited damage. Under 0.20g PGA, the hysteresis loop did not follow a characteristic S shape because of the plastic deformation of coupling beams. Areas of the hysteresis loops increased as PGA increased, indicating that the test model suffered more obvious damage. The hysteretic characteristics are consistent with the observed damage development process. Under the pseudo-dynamic tests, the test model reached its peak lateral load in the positive direction but did not in the negative direction. The strength of the test model dropped slowly at the postpeak stage and F_{EK} was reduced to 77.0% and 80.5% of the peak load in the positive and negative direction, respectively, at $1/50$ drift, showing excellent ductile behavior.

Figure A8 plots the lateral deformation distribution along the height when the top displacement reached its peak values in the positive and negative directions under various load conditions. It is observed that the lateral deformation distribution presented a flexural mode with interstory drifts increasing from the first story to the third story. The interstory drift ratios of the second and third stories were nearly identical under different load conditions and significantly larger than that of the first story.

Strength and deformation capacity

Table 1 summarizes F_{EK} and θ at specific states, where the nominal yield point was determined based on the concept of equal energy of an idealized elastoplastic system,³² the peak load point corresponded to the point with maximum lateral load on the skeleton curve, and the ultimate point was taken

Table 1. Strength and deformation capacity of test model

Loading direction	Nominal yield point			Peak load point			Ultimate point			D_u
	$F_{EK,y}$, kN	θ_y	η	$F_{EK,p}$, kN	θ_p	η	$F_{EK,u}$, kN	θ_u	η	
Positive	1701.8	$1/247$	0.35	2040.9	$1/160$	0.26	1734.8	$1/59$	0.08	4.2
Negative	1641.2	$1/252$	0.35	1934.3	$1/115$	0.19	1644.2	$1/50$	0.07	5.0

Note: D_u = displacement ductility ratio; $F_{EK,p}$ = base shear force at peak load; $F_{EK,y}$ = base shear force at nominal yield load; $F_{EK,u}$ = base shear force at ultimate load; θ_p = drift ratio at peak load; θ_y = drift ratio at nominal yield load; θ_u = drift ratio at ultimate load; η = stiffness degradation coefficient. 1 kN = 0.225 kip.

as the point corresponding to a 15% reduction in lateral-load resistance. In Table 1, the displacement ductility ratio is defined as $D_u = \theta_u / \theta_y$. The peak load drift ratios for the positive and negative directions were $1/_{160}$ and $1/_{115}$, respectively. The ultimate drift ratios for the positive and negative directions were $1/_{59}$ and $1/_{50}$, respectively, which are much larger than $1/_{120}$, satisfying the requirement for deformation capacity in Chinese codes.^{25,26} The strength (peak load) of the test model was approximately 1.3 times the maximum base shear force under 0.40g PGA, indicating that an adequate safety margin was achieved under seismic design intensity 8.

Stiffness degradation

The lateral stiffness of the test model K is defined as $K = F_{EK} / u$. The stiffness degradation coefficient η is calculated as $\eta = K / K_0$, where K_0 is the initial stiffness measured by a quasi-static test before pseudodynamic tests (Fig. A3). The stiffness after each pseudodynamic test was measured by one complete cycle of response with a top lateral displacement amplitude of 2 mm (0.08 in.). Stiffness degradation curves for the pseudodynamic and quasi-static tests are shown in Fig. 7, and values of η under specific states are given in Table 1.

Stiffness decreased by 5%, 19%, 62%, and 77% after the 0.07g, 0.20g, 0.40g, and 0.62g pseudodynamic tests, respectively. The structure period increased as the stiffness degraded, resulting in sparser time-history responses with the seismic intensity increasing (Fig. 6). In the early loading stage, the stiffness degraded rapidly, owing to the extensively developing cracks and damage. However, the degradation slowed down later because no new cracks developed.

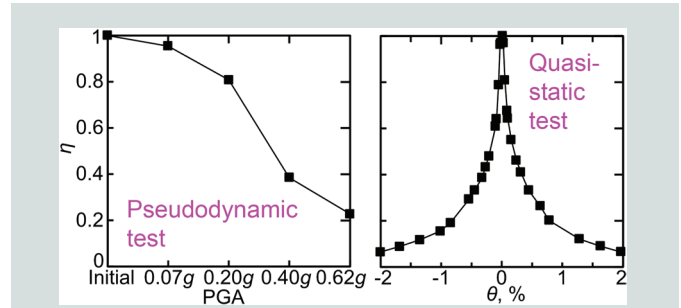


Figure 7. Stiffness degradation curves. Note: g = acceleration due to gravity; PGA = peak ground acceleration; θ = top drift ratio; η = stiffness degradation coefficient.

Performance level and damage state evaluation

Damage states of the test model can be evaluated intuitively by global behavior, such as interstory drift and observed damage phenomena. The Chinese code GB 50011-201025 classifies damage states of shear wall structures into five levels based on the interstory drift ratio θ_{is} . For instance, $\theta_{is} < 1/_{1000}$, $1/_{1000} < \theta_{is} < 1/_{500}$, $1/_{500} < \theta_{is} < 1/_{250}$, $1/_{250} < \theta_{is} < 1/_{133}$, and $\theta_{is} > 1/_{120}$ correspond to no damage, slight damage, moderate damage, severe damage, and collapse, respectively. FEMA 356³⁵ synthetically evaluates building performance levels based on transient and permanent drifts, damage degree of vertical and horizontal elements, and damage degree of nonstructural elements.

Table 2 summarizes damage states and performance levels of the test model under various PGA according to GB 50011-2010 and FEMA 356. Note that although the maxi-

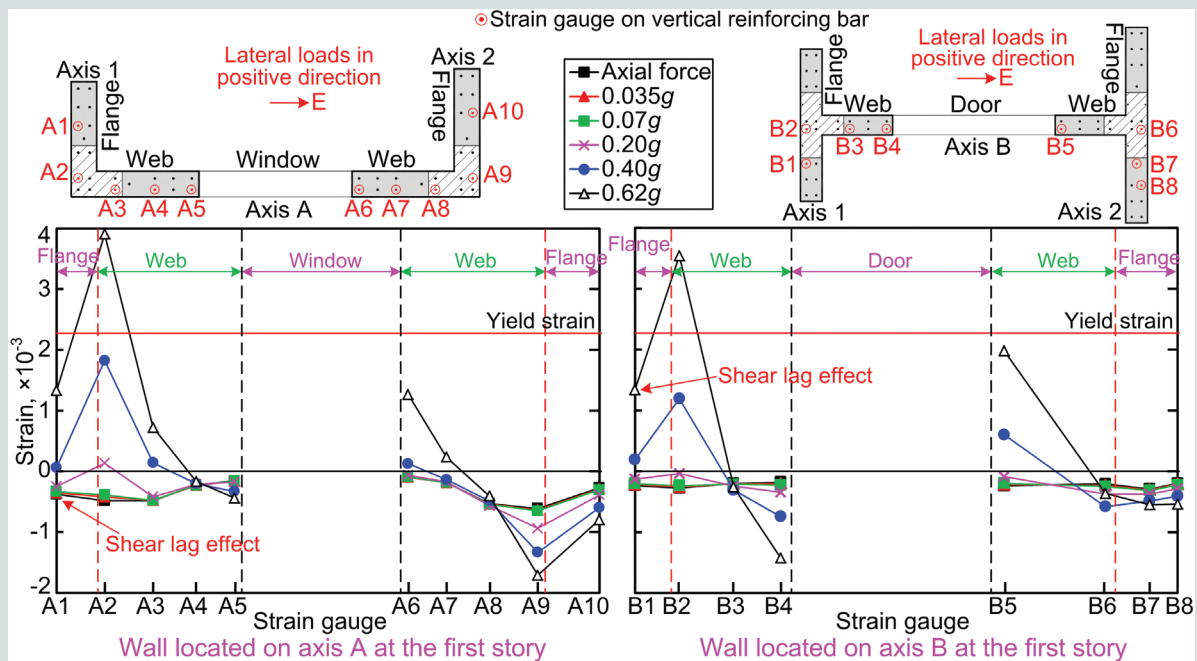


Figure 8. Vertical reinforcing bar strain distributions along wall pier bottom section under peak top displacement of various peak ground accelerations. Note: g = acceleration due to gravity.

imum interstory drift exceeded $1/120$ under $0.62g$ PGA, the test model did not visually collapse and could continue to resist gravity and lateral loads with slight cracking in wall piers and slight strength degradation in the positive direction. The damage states under $0.07g$, $0.20g$, and $0.40g$ PGA indicated that performance objective grade 2 of performance-based seismic design in Chinese code was maintained under seismic design intensity 8.²⁵ Under a rare earthquake of seismic fortification intensity 8 (that is, maximum considered earthquake), the test model was under moderate damage or intermediate occupancy performance level, showing an excellent seismic performance.

Reinforcing bar strain development






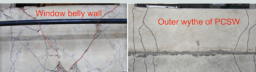
Figure 8 shows vertical reinforcing bar strain distributions along wall piers at the test model bottom, which were con-

sistent with the plane section assumption,³² indicating that vertical reinforcing bars in vertical cast-in-place segments and precast concrete walls could work together. Strains in vertical reinforcing bars adjacent to the web were much larger than those in the vertical reinforcing bars farther from the web, and the former yielded sooner than the latter, indicating that a significant shear lag effect existed in the flange, which was observed in some existing T-shaped shear wall tests.^{36,37} The influence of shear lag on T-shaped wall strength should be carefully considered in design.

The reinforcing bar strain development and yield sequence is shown in Table 3.

- No reinforcing bar yielded under $0.07g$ and $0.20g$ PGA.
- Under $0.40g$ PGA, most coupling beam longitudinal

Table 2. Performance level and damage state evaluation of test model

Peak ground acceleration	Drift ratio	Observed structural damage on coupling beam, wall, and diaphragm	Observed nonstructural damage on window belly wall and outer wythe of precast concrete sandwich wall	GB 50011-2010 damage state	FEMA 356 performance level		
					SPL	NSPL	TBPL
$0.07g$	$1/3011$ transient, negligible permanent	No visible crack	No visible crack	No damage	OP	OP N-A	OP 1-A
$0.20g$	$1/899$ transient, $1/17351$ permanent	 Coupling beams suffered cracks < 0.1 mm	 Window belly walls (partition) suffered cracks < 0.2 mm	Slight damage	OP	OP N-A	OP 1-A
$0.40g$	$1/268$ transient, $1/10975$ permanent	 Coupling beams suffered cracks < 0.5 mm and no spalling; minor hairline cracking of walls	 Window belly walls suffered shear-inclined cracks < 0.6 mm	Moderate damage	IO S-1	IO N-B	IO 1-B
$0.62g$	$1/111$ transient, $1/1982$ permanent	 Coupling beams suffered shear cracks < 1.5 mm and slight crushing; minor cracking of walls. Slabs suffered minor cracking	 Window belly walls suffered severe cracking and crushing; outer wythes (cladding) of precast concrete sandwich wall suffered minor cracking	Collapse, but could continue to support gravity loads and resist lateral loads	LS S-3	LS N-C	LS 3-C

Note: Transient drift is the maximum interstory drift under consistent peak ground acceleration, and permanent drift is the residual drift when F_{EK} was unloaded to zero. F_{EK} = base shear force; g = acceleration due to gravity; IO = immediate occupancy; LS = life safe; NSPL = nonstructural performance level; OP = operational; SPL = structural performance level; TBPL = target building performance level. 1 mm = 0.0394 in.

Table 3. Maximum tension strains of reinforcing bars under various peak ground acceleration, $\mu\epsilon$

Peak ground acceleration	First story				Second story				Third story
	WVR	BLR	BS	SNR	WVR	BLR	BS	SNR	WVR
0.07g	C	357	15	25	C	191	9	88	C
0.20g	297	1507	94	67	C	928	22	179	C
0.40g	4497	3245	462	1783	472	4924	811	1139	635
0.62g	8103	*	2421	2993	1309	*	4236	1792	714

Note: BLR = coupling beam longitudinal reinforcing bar; BS = coupling beam stirrup; C = in compression; g = acceleration due to gravity; SNR = slab negative reinforcing bar in the cast-in-place concrete topping; WVR = wall vertical reinforcing bar.

* Reinforcing bar strain exceeded 10,000 $\mu\epsilon$.

reinforcing bars at the first and second story and individual extreme wall vertical reinforcing bars at the first story yielded by tension.

- Under 0.62g PGA, longitudinal reinforcing bars of all coupling beams and the stirrups of most coupling beams at the first and second story yielded by tension, while extreme vertical reinforcing bars of most wall piers and SNR bars in the cast-in-place concrete topping at the first story also yielded by tension.
- The coupling beam longitudinal reinforcing bars, wall pier vertical reinforcing bars, and coupling beam stirrups yielded in turn, indicating that the design concepts “strong wall pier and weak coupling beam” and “strong shear and weak bending of coupling beam” were achieved.

Conclusion

This paper investigated the seismic behavior of an emulative precast concrete shear wall systems with grouted couplers, in which wall vertical reinforcing bars are spliced by grouted couplers, adjacent precast concrete panels are connected by vertical cast-in-place segments, and precast concrete slabs with cast-in-place concrete toppings are used as diaphragms tying vertical members together. The following conclusions are drawn from this study:

- Damage to the test model was concentrated in coupling beams and window belly walls in the lateral-load input direction, characterized by severe cracking and concrete spalling, while wall piers suffered extensive cracking within 2.0 m (6.6 ft) of the foundation. The coupling beam longitudinal reinforcing bars, wall pier vertical reinforcing bars, and coupling beam stirrups yielded in turn. The seismic-resisting concepts “strong wall pier and weak coupling beam” as well as “strong shear and weak bending of coupling beam” were achieved.
- The precast concrete shear wall system with grouted couplers exhibited excellent seismic performance. In

particular, under 0.07g, 0.20g, 0.40g, and 0.62g PGA, the test model experienced no damage, slight damage, moderate damage, and collapse state, respectively, according to GB 50011-2010, and met the operational, immediate occupancy, and life safety performance levels, respectively, as per FEMA 356, with a maximum interstory drift ratio of $1/_{3341}$, $1/_{899}$, $1/_{268}$, and $1/_{111}$, and lateral stiffness decreasing by 5%, 19%, 62%, and 77%, respectively. The test model showed excellent deformation capacity, with ultimate drift ratios approaching 0.02.

- The performance of joints connecting precast concrete members was specially identified in this paper, and no visible damage concentrated on these joints, indicating that these joints were strong enough to ensure that the behavior of the precast concrete shear wall system with grouted couplers would as if it were monolithic.
- Window belly walls, which were precast with wall piers as a whole, significantly affected crack patterns in the lower coupling beams under large drift, though weak construction details, such as infilling polystyrene blocks in window belly walls or no spliced reinforcement between coupling beams and window belly walls, were utilized. The influence of window belly walls on the stiffness and failure mode of the structure, as well as the composite effect between the window belly wall and the lower coupling beams, should be carefully considered in structure design.
- Different crack distributions formed on the outer and inner wythes of precast concrete sandwich walls, revealing that a low degree of in-plane composite action between these two wythes was achieved by the proposed connection details. The influence of the outer wythe can be neglected in structure design, but FRP connectors and reinforcing bars within the severe cracking zone of the outer wythe should be well designed and detailed to prevent failing of the outer wythe under large drift.
- Under the test loading conditions, the superimposed concrete slab without protruding reinforcing bars could work

as a diaphragm-emulated slab with protruding reinforcing bars, with no crack and slippage developing around both types of slab supports, and no torsion of the test model. The constraint effect from wall piers significantly contributed to preventing the slab supports from severe plastic tension deformation; therefore, wall piers should be designed with adequate lateral stiffness in superimposed slabs without protruding reinforcing bars.

Acknowledgments

This work was sponsored by Beijing Wanke Ltd. and Beijing Residential Building Design and Research Institute. Beijing Architecture Design and Research Institute helped design the prototype structure. China Construction First Building Ltd. helped construct the test model. The grouted sleeves and grout used in the test model were sponsored by Beijing Sida Jianmao Technology Development Ltd. Other professors and graduate students in the high-rise structure research group of Tsinghua University in Beijing, China, assisted in some laboratory work. The authors wish to thank the whole research team for their assistance in the experimental program.

References

- Soudki, K. A., S. H. Rizkalla, and B. LeBlanc. 1995. "Horizontal Connections for Precast Concrete Shear Walls Subjected to Cyclic Deformations, Part 1: Mild Steel Connections." *PCI Journal* 40 (4): 78–96.
- Pekau, O. A., and D. Hum. 1991. "Seismic Response of Friction Jointed Precast Panel Shear Walls." *PCI Journal* 36 (2): 56–71.
- Schultz, A. E., M. K. Tadros, X. Huo, and R. A. Magaña. 1994. "Seismic Resistance of Vertical Joints in Precast Shear Walls." In *FIP '94 XII Congress May 29–June 2, Washington, D.C.*, Vol. 1, E23–E27. London, U.K.: Structural Engineers Trading Organisation Ltd.
- Priestley, M. J. N., S. Sritharan, J. R. Conley, and S. Pampanin. 1999. "Preliminary Results and Conclusions from the PRESSS Five-Story Precast Concrete Test Building." *PCI Journal* 44 (6): 42–67.
- Kurama, Y. C. 2005. "Seismic Design of Partially Post-tensioned Precast Concrete Walls." *PCI Journal* 50 (4): 100–125.
- Einea, A., T. Yamane, and M. K. Tadros. 2005. "Grout-Filled Pipe Splices for Precast Concrete Construction." *PCI Journal* 40 (1): 82–93.
- Crisafulli, F. J., J. I. Restrepo, and R. Park. 2002. "Seismic Design of Lightly Reinforced Precast Concrete Rectangular Wall Panels." *PCI Journal* 47 (4): 104–121.
- Li, N., J. Qian, L. Ye, and S. Liu. 2016. "Tests on Seismic Behavior of Precast RC Shear Walls with Vertical Rebar Splicing by Pressed Sleeve." *Journal of Building Structures* 37 (1): 31–40.
- Sun, J., H. Qiu, and Y. Lu. 2016. "Experimental Study and Associated Numerical Simulation of Horizontally Connected Precast Shear Wall Assembly." *The Structural Design of Tall and Special Buildings* 25 (13): 659–678.
- Sayadi, A. A., A. B. A. Rahman, M. Z. B. Jumaat, U. J. Alengaram, and S. Ahmad. 2014. "The Relationship between Interlocking Mechanism and Bond Strength in Elastic and Inelastic Segment of Splice Sleeve." *Construction and Building Materials* 55: 227–237.
- Ling, J. H., A. B. A. Rahman, I. S. Ibrahim, and Z. A. Hamid. 2017. "An Experimental Study of Welded Bar Sleeve Wall Panel Connection under Tensile, Shear, and Flexural Loads." *International Journal of Concrete Structures and Materials* 11 (3): 525–540.
- Henin, E., and G. Morcou. 2015. "Non-proprietary Bar Splice Sleeve for Precast Concrete Construction." *Engineering Structures* 83: 154–162.
- Ling, J. H., A. B. A. Rahman, and I. S. Ibrahim. 2014. "Feasibility Study of Grouted Splice Connector under Tensile Load." *Construction and Building Materials* 50: 530–539.
- Park, R. 2002. "Seismic Design and Construction of Precast Concrete Buildings in New Zealand." *PCI Journal* 47 (5): 60–75.
- CMC (China Ministry of Construction). 2014. *Technical Specification for Precast Concrete Structures*. JGJ 1-2014. Beijing, China: CMC.
- Han, J. 2005. "An Experimental Study on Dry-connections for Precast Concrete Walls." MS thesis, Seoul National University, Seoul, South Korea. Xu, Z. 2016. "Experimental Study on Seismic Behavior of Precast Concrete Shear Walls Base on New-Type Connection." MS thesis, Tongji University, Shanghai, China.
- Peng, Y., J. Qian, and Y. Wang. 2016. "Cyclic Performance of Precast Concrete Shear Walls with a Mortar-Sleeve Connection for Longitudinal Steel Bars." *Materials and Structures* 49 (6): 2455–2469.
- Qian, J., X. Yang, H. Qin, Y. Peng, J. Zhang, and J. Li. 2011. "Tests on Seismic Behavior of Pre-cast Shear Walls with Various Methods of Vertical Reinforcement Splicing." *Journal of Building Structures* 32 (6): 51–59.
- Zhang, W., J. Qian, K. Chen, H. Qin, G. Liu, and J. Li. 2011. "Tests on Seismic Behavior of Pre-cast Shear Walls with Vertical Distributed Reinforcement Spliced

- by a Single Row Connecting Rebars.” *Building Structure* 41 (2): 12–16.
20. Zhang W., J. Qian, J. Yu, H. Qin, and G. Liu. 2012. “Tests on Seismic Behavior of Precast Shear Walls with Cast-in-Situ Boundary Elements and Vertical Distributed Reinforcement Spliced by a Single Row of Steel Rebars.” *China Civil Engineering Journal* 45 (10): 89–97.
 21. Niu, P. 2016. “Low Reversed Cyclic Loading Test of Precast Concrete Shear Walls under High Axial Compressive Ratio.” MS thesis, Tongji University, Shanghai, China.
 22. Qian, J., Y. Hu, Z. Zhao, S. Feng, Y. Zhang, G. Liu, Z. Pan, and J. Li. 2014. “Experimental Study on Seismic Behavior of Assembled Monolithic Coupling Beams.” *China Civil Engineering Journal* 47 (9): 9–20.
 23. Zhang, W., X. Jiang, B. Zhang, H. Qin, and Y. Zhang. 2013. “Experimental Research on Seismic Behavior of Coupling Beams of Assembly Integrated Coupled Shear Walls.” *World Earthquake Engineering* 29 (4): 26–32.
 24. CMC. 2010. *Code for Seismic Design of Buildings*. GB 50011-2010. Beijing, China: CMC.
 25. CMC. 2010. *Code for Design of Concrete Structures*. GB 50010-2010. Beijing, China: CMC.
 26. Han, W., Z. Zhao, and J. Qian. 2017. “Test Report on a Precast Shear Wall Structure with Rebars Spliced by Grouted Couplers.” Technical report, Tsinghua University, Beijing, China.
 27. Pan, P., T. Wang, and M. Nakashima. 2015. *Development of Online Hybrid Testing: Theory and Applications to Structural Engineering*. Oxford, U.K.: Elsevier Science and Technology.
 28. Qian, G., and F. Zhu. 2010. “Comparison of Seismic Behavior of Shear Wall Structures with Dual and Deep Coupling Beams.” *China Civil Engineering Journal* 43 (S1): 211–216.
 29. Fenwick, R. C., and L. M. Megget. 1993. “Elongation and Load Deflection Characteristics of Reinforced Concrete Members Containing Plastic Hinges.” *Bulletin of the New Zealand National Society for Earthquake Engineering* 26 (1): 28–41.
 30. Fenwick, R. C., and B. J. Davidson. 1995. “Elongation in Ductile Seismic-Resistant Reinforced Concrete Frames.” ACI Special Publication 157. Farmington Hills, MI: ACI (American Concrete Institute).
 31. Guo, Z. 2014. *Principles of Reinforced Concrete*. Oxford, U.K.: Butterworth-Heinemann.
 32. Peng, B. H. H. 2009. “Seismic Performance Assessment of Reinforced Concrete Buildings with Precast Concrete Floor Systems.” PhD thesis, University of Canterbury, Christchurch, New Zealand.
 33. Matthews, J. G. 2004. “Hollow-Core Floor Slab Performance Following a Severe Earthquake.” PhD thesis, University of Canterbury, Christchurch, New Zealand.
 34. American Society of Civil Engineers. 2000. *Prestandard and Commentary for the Seismic Rehabilitation of Buildings*. FEMA-356). Washington, DC: FEMA (Federal Emergency Management Agency).
 35. Thomsen, J. H., and J. W. Wallace. 2004. “Displacement-Based Design of Slender Reinforced Concrete Structural Walls—Experimental Verification.” *Journal of Structural Engineering* 130 (4): 618–630.
 36. Zhang, Z., and B. Li. 2016. “Seismic Performance Assessment of Slender T-Shaped Reinforced Concrete Walls.” *Journal of Earthquake Engineering* 20 (8): 1342–1369.

Notation

- d = reinforcing-bar diameter
- D_u = displacement ductility ratio
- F_A = lateral force applied by actuators
- $F_{A,max}$ = maximum lateral force applied by actuators
- F_{EK} = base shear force
- $F_{EK,max}$ = maximum base shear force
- $F_{EK,p}$ = base shear force at peak load
- $F_{EK,u}$ = base shear force at ultimate load
- $F_{EK,y}$ = base shear force at nominal yield load
- F_H = horizontal component of inclined prestress
- g = acceleration due to gravity
- K = lateral stiffness of the test model
- K_0 = initial lateral stiffness

- L_0 = initial length of prestressing tendons
- N = applied axial load
- u = lateral displacement of the third-story slab
- δ = relative force
- Δ = lateral displacement at loading beams
- ΔN = increment of applied axial load
- θ = top drift ratio
- θ_{is} = interstory drift ratio
- θ_{max} = maximum top drift ratio
- θ_p = drift ratio at peak load
- θ_u = drift ratio at ultimate load
- θ_y = drift ratio at nominal yield load
- η = stiffness degradation coefficient

About the authors



Wenlong Han is a PhD candidate in the Department of Civil Engineering at Tsinghua University in Beijing, China, where he also received his BEc. His research mainly focuses on precast concrete shear wall structures.



Zuozhou Zhao, PhD, is an associate professor in the Department of Civil Engineering at Tsinghua University, where he received his BEc and MEc. He received his doctoral degree in earthquake engineering from the University of Hong Kong. His

research interests include reinforced precast concrete structures, composite structures, and seismic design and analysis of structures.



Jiaru Qian is a professor in the Department of Civil Engineering at Tsinghua University, where he received his BEc in 1970. He has served as an expert on the Chinese national review committee on seismic fortification of out-of-code high-rise buildings since 2006. He

is a principal member of drafting committees for several Chinese primary design codes on precast concrete structures. His current research interests include reinforced precast concrete structures, composite structures, and seismic design and analysis of structures.

Abstract

This paper presents an experimental study of a three-story, full-scale precast concrete shear wall structure in which vertical reinforcing bars in the walls were spliced by grouted couplers, adjacent precast concrete panels were connected by vertical segments, and precast concrete slabs with cast-in-place concrete topping were used as diaphragms tying vertical members together. Critical joints, such as horizontal and vertical wall-to-wall joints, window belly wall connections, slab-to-wall joints, slab-to-slab joints, and precast concrete sandwich panel connections, were designed and verified. Results of a series of pseudodynamic and quasi-static tests showed that the test model exhibited excellent seismic performance and failed in the desired mode. The adopted joints were strong enough to ensure behavior of the precast concrete shear wall with grouted coupler systems as if monolithic. The performance levels and damage states of the test model under various seismic intensities were evaluated according to Chinese code GB 50011-2010 and FEMA 356. Particular attention was placed on the influence of window belly walls, the performance of precast concrete sandwich walls, and the performance of superimposed concrete slabs with different slab-to-wall joints.

Keywords

Connection, grouted coupler, quasi-static test, sandwich wall, shear wall structure, substructure pseudo-dynamic test, superimposed concrete slab support, window belly wall.

Review policy

This paper was reviewed in accordance with the Precast/Prestressed Concrete Institute's peer-review process.

Reader comments

Please address any reader comments to *PCI Journal* editor-in-chief Emily Lorenz at elorenz@pci.org or Precast/Prestressed Concrete Institute, c/o *PCI Journal*, 200 W. Adams St., Suite 2100, Chicago, IL 60606.